Toxicity and structure-activity relationship (SAR) of α, β-dehydroamino acids against human cancer cell lines

Romeu A. Videira[a], Paula B. Andrade[a], Luís S. Monteiro[a], Patrícia Valentão[a], Paula M.T. Ferreira[b], David M. Pereira[a*]

[a]REQUIMTE/LAQV, Laboratório de Farmacognosia, Departamento de Química, Faculdade de Farmácia, Universidade do Porto, Rua de Jorge Viterbo Ferreira, Nº 228, 4050-213, Porto, Portugal. (e-mail addresses: Romeu A. Videira – rvideira@ff.up.pt; Paula A. Andrade – pandrade@ff.up.pt; Patrícia Valentão - valentao@ff.up.pt; David M. Pereira - dpereira@ff.up.pt)

[b]Centre of Chemistry, University of Minho, Campus de Gualtar, 4710-057 Braga, Portugal. (e-mail addresses: Luís S. Monteiro - monteiro@quimica.uminho.pt; Paula M.T. Ferreira - pmf@quimica.uminho.pt>)

* Corresponding author.

David M. Pereira
REQUIMTE/LAQV, Laboratório de Farmacognosia, Departamento de Química
Faculdade de Farmácia, Universidade do Porto, Rua de Jorge Viterbo Ferreira, Nº 228, 4050-213, Porto, Portugal
E-mail: dpereira@ff.up.pt
Telephone:+351 220428655**; Fax:** +351 226093390

Keywords: Dehydroamino acids; Toxicological profile, Apoptosis; Caspases; Therapeutic agents; **structure-activity relationship (SAR)**

Abstract

A library of *N*-protected dehydroamino acids, namely dehydroalanine, dehydroaminobutyric acid and dehydrophenylalanine derivatives, was screened in three human cancer cell lines [(lung (A549), gastric (AGS) and neuroblastoma (SH-SY5Y)] in order to characterize their toxicological profile and identify new molecules with potential anticancer activity. Results showed *N*-protected dehydrophenylalanine and dehydroaminobutyric acid derivatives have no or low toxicity for all tested cell lines. The *N*-protected dehydroalanines exhibit significant toxic effects and the AGS and SH-SY5Y cells were significantly more vulnerable than A549 cells. Four α,β-dehydroalanine derivatives, with IC_{50}< 62.5 μM, were selected to investigate the pathways by which these compounds promote cell death. All compounds, at their IC_{50} concentrations, were able to induce apoptosis in both AGS and SH-SY5Y cell lines. In both cell lines, loss of mitochondrial membrane potential (ΔΨm) was found and caspase activity was increased, namely endoplasmic reticulum-resident caspase-4 in AGS cells and caspase-3/7 in SH-SY5Y. When evaluated in a non-cancer cell line, the molecules displayed no to low toxicity, thus suggesting some degree of selectivity for cancer cells. The results indicate that α,β-dehydroalanine derivatives can be considered a future resource of compounds able to work as anticancer drugs.

1. Introduction

α,β-Dehydroamino acids are non-coded amino acids, characterized by one double bound between the C_α and C_β atoms. α,β-Dehydroamino can be found in peptides isolated from bacteria, fungi, marine invertebrates and higher plants (Siodłak, 2015). In general, the presence of one or more α,β-dehydroamino acids in a polypeptide chain has strong impact, not only on the secondary structure adopted, but also on their biological behaviour, including antibacterial, antifungal and antitumor activities (Siodłak, 2015; Rudresh et al., 2004; Gupta and Chauhan, 2011). The current natural α,β-dehydroamino acids, detected in thousands of different polypeptides, comprise 37 distinct molecular species; however, not all of them can be derived from proteinogenic α,β-amino acids.

It has been shown that the bioactivity of natural dehydropolypeptides is largely dependent on the presence of α,β-dehydroamino acid, as well as on their absolute configuration (*E*/*Z* isomerism) (Ward et al., 1999; Bonnard et al., 2007). Therefore, α,β-dehydroamino acids may be produced/incorporated in the polypeptides by highly regulated biochemical pathways, preserved during the evolutionary process by the adaptive advantages that these natural products should confer to the producing organisms. In fact, organisms with different levels of complexity exhibit the biosynthetic route of lanthipeptides, where dehydroalanine and dehydroaminobutyric acid are produced, in the first step, by a post-translationally dehydration of serine and threonine, respectively. Subsequently, the thiol of a Cys is added across the carbon–carbon double bond of these dehydroamino acids to generate the characteristic lanthionine and methyllanthionine thioether-bridged structures (Repka et al. 2017). Thus, lanthipeptides are polycyclic peptides belong to a growing family of secondary metabolites known as ribosomally synthesized and post-translationally modified peptides (Arnison et al. 2013). The broad spectrum of bioactivity and applications found

among the known natural compounds containing α,β-dehydroamino acid residues have driven the development of methods for the chemical synthesis of dehydroamino acids derivatives with selective biological profile for biomedical applications. Since dehydroamino acids cannot be incorporated using standard peptide synthesis methods, several strategies were developed to pursue that goal. One such strategy, which mimics the lanthipeptides biosynthetic pathway, relies on the incorporation of one masked amino acid into a polypeptide precursor, followed by their chemoselective dehydration (Okeley et al., 2000; Morrison et al., 2015). In our laboratory we developed a simple and high yielding procedure to prepare α,β-dehydroamino acid derivatives from β-hydroxyamino acids by treatment with *tert*-butylpyrocarbonate $(Boc)_2O$, 4-dimethylaminopyridine (DMAP), followed by treatment with tetramethylguanidine (TMG) (Ferreira et al.,1998; Ferreira et al.,1999; Ferreira et al., 2007). In addition to their intrinsic bioactivity, these compounds can be used either as building blocks for the synthesis of dehydropolypeptides, as well as substrates to prepare new compounds designed to target specific biological targets.

In the present work, the toxicological profile of nineteen α,β-dehydroamino acids, with different *N*-protecting groups, was characterized using three distinct human cancer cell lines and one non-cancer cell line. Cell death mechanisms triggered by the compounds with higher toxicity were also investigated, considering the effects on cell viability, membrane integrity, cell morphology, caspase activity and mitochondrial membrane potential.

2. Material and methods

2.1. Compounds synthesis and estimation of octanol-water partition coefficients

The synthesis of the methyl esters of dehydroamino acids *N*-protected with benzoyl (Bz), 4-nitrobenzoyl [Bz(4-NO_2)], 4-nitrobenzyloxycarbonyl [Z(NO_2)], 4-methoxybenzoyl [Bz(OMe)], naphthaloyl (Naph), quinoxalyl (Qnx), 4-toluenesulfonyl (Tos), 4-nitrobenzenesulfonyl (Nosyl) and *tert*-butoxycarbonyl (Boc) was already described. (Ferreira et al., 1998; Ferreira et al., 1999; Ferreira et al., 2007; Ferreira et al., 2001; Ferreira et al., 2003; Ferreira et al., 2008).

The partition coefficient between water and *n*-octanol (Log P) of each compound was estimated using Molinspiration Cheminformatics software (Molinspiration, Slovensky Grob, Slovak Republic, 2017, http://www.molinspiration.com), as a sum of fragment-based contributions and correction factors, and it is used as quantitative descriptor of compound lipophilicity (Cedrón et al., 2005).

2.2.Cell culture

Three distinct human cancer cell lines were used in this research: gastric carcinoma (AGS; Sigma-Aldrich, St. Louis, MO, USA), neuroblastoma (SH-SY5Y; ATCC, Barcelona, Spain) and lung carcinoma (A549; ECACC, Porton Down Salisbury, UK). The human fetal lung fibroblast cell line MRC-5 (ECACC, Porton Down Salisbury, UK) was used as non-cancer cell model. Cell lines were cultured as monolayer at 37 °C in a humidified incubator with 5% carbon dioxide. AGS and SH-SY5Y cells were grown in glutamine-enriched Dulbecco's Modified Eagle Medium (DMEM), supplemented with 1% streptomycin/penicillin and 10% foetal bovine serum (Gibco®), while A549 and MRC-5 cells were grown, respectively, in DMEM/F-12 and MEM-GlutaMax, supplemented with 1% streptomycin/penicillin and 10% foetal bovine serum. For subculture, cells were washed with Hank's buffered salt solution (HBSS), treated with 0.25% Trypsin-EDTA solution (Sigma, St. Louis, MO) for 3 min at 37 °C,

resuspended in 5 mL of culture medium and centrifuged at 390 *g* for 4 min. The supernatant was removed and the cell pellet was resuspended in culture medium. Subculture ratio was usually 1:3 for SH-SY5Y cells and 1:5 for ASG and A549 cells. Cell passages were kept low for all cell lines, with a maximum of 12 passages.

2.3.Cell viability and membrane integrity

Cell viability was evaluated using the MTT [(3-(4,5-dimethylthiazol-2-yl)-2,5-diphenyltetrazolium] reduction assay, while membrane integrity was assessed by the lactate dehydrogenase (LDH) release assay, as previously described [Pereira et al., 2014]. Briefly, cells were seeded in 96-well microplates at a density of 15,000, 30,000, 10,000 and 20,000 cells/well for AGS, SH-SY5Y, A549 and MRC-5 cells, respectively, and placed at 37 °C in a CO_2 incubator. After 24 h cells reached 70–80% confluence and were incubated with the dehydroamino acid derivatives at different concentrations (up to 62.5 μM) or with DMSO (vehicle), at 37 °C for 24 h, after which the MTT and LDH assays were conducted, as described below.

MTT (0.5 mg/mL final concentration) was added to each well and the plate was incubated for 2 h, at 37 °C. The formazan was dissolved with 200 μL of a DMSO:isopropanol mixture (3:1, V:V) and quantified spectrophotometrically at 560 nm using a microplate reader (Multiscan GO, Thermo Scientific). Results were expressed as percentage of control and IC_{50} values were determined from the plots of cell viability data against α,β-dehydroamino acid derivatives concentration.

LDH activity was evaluated spectrophotometrically following NADH oxidation at 340 nm during 3 min, using a microplate reader (Multiscan GO, Thermo Scientific). The reaction was conducted using 50 μL of cell-free supernatant of extracellular medium or 25 μL of supernatant of cell lysates into phosphate buffer (50 mM KH_2PO_4, pH 7.4),

supplemented with 10 μM pyruvate and 300 μM of NADH. LDH release in each well was determined by the ratio between LDH activity in extracellular medium and LDH activity of controls treated with lysis solution (1% Triton X-100 in 10 mM phosphate buffer, pH = 7.2). Results were expressed as fold increase relative to DMSO-treated cells (vehicle-treated controls).

2.4.Cell lipid extraction, phospholipids and cholesterol quantification

Total lipids of A549, AGS, SH-SY5Y and MRC-5 cells were extracted by using a double extraction procedure with a solvent combination of methanol/chloroform/water at final proportions of 2:1:0.8 (v/v/v), as previously described (Monteiro-Cardoso et al., 2014). Briefly, a volume of cell suspension corresponding to 2 mg of protein was reconstituted in 0.8 mL aqueous buffer, mixed with 2 mL methanol and 1 mL chloroform and then centrifuged at 2,000 *g* for 5 min at 4 °C. Supernatant was collected and an additional volume of 1 mL chloroform and 2 mL water were added to supernatant following vigorous mixing. Samples were centrifuged at 2000 *g* for 5 min at 4◦C, in order to obtain a two-phase system: an aqueous top phase and an organic bottom phase from which lipids were collected. The pellet obtained in the first centrifugation was used to perform lipid re-extraction. The extracts were dried in a nitrogen stream and used to quantify the cholesterol and phospholipid contents.

Cholesterol of total lipid extracts was quantified according to Liebermann-Burchard procedures and phospholipids by phosphorus assay after acid hydrolyses, as previously described (Monteiro-Cardoso et al., 2014).

2.5.Caspases assays

Caspase-3/7 protease activity was evaluated fluorometrically, by measuring the ability of cell lysates to cleave the proluminescent DEVD peptide-rhodamine 110 substrate (Z-DEVD)2-R110;Caspase-Glo®kit, Promega, Madison USA), as suggested by the manufacturer. AGS and SH-SY5Y were seeded in 96-well white plates, as previously described for MTT and LDH. After 24 h cells were incubated with dehydroamino acid derivatives at IC_{50} concentrations, or with either 250 nM staurosporine (positive control) or vehicle (DMSO), for 8 h, at 37 °C. After this period, 50% of cell medium was removed and similar volume of caspase-3/7 substrate was added. Plates were incubated in a microplate reader (Synergy H1, BioTek) and the luminescent signal was measured at different time points, up to 120 min. Results were expressed as fold increase in luminescence relative to DMSO-treated cells (vehicle-treated controls).

Caspase-4 activity was assessed by the ability of cell lysates to cleave specific Z-AFC peptide substrate (Innovagen, Lund, Sweden) and to produce a fluorescent compound with emission at 505 nm under excitation at 400 nm. AGS and SH-SY5Y cells were seeded in 96-well black plates, as previously described for MTT and LDH assays, and allowed to attach for 24 h. Afterwards, cells were incubated with α,β-dehydroamino acid derivatives at IC_{50} concentrations, or with 1 mM palmitic acid (positive control) or vehicle (DMSO), for 8 h, at 37 °C. Supernatants were removed, caspase-4 substrate (50 μM) was added and plates were incubated for 150 min, at 37 °C. Fluorescence (excitation: 400 nm; emission: 505 nm) was determined in a microplate reader (Synergy H1, BioTek) at different time points, up to 120 min. Results were expressed as fold increase relative to DMSO-treated cells (controls).

For the assessment of caspase-9 activity, AGS and SH-SY5Y cells were seeded in 6-well plates at a cell density of 75,000 and 550,000 cells/well, respectively, and placed at 37 °C in a CO_2 incubator. After 24 h cells were incubated with α,β-dehydroamino acid

derivatives at IC_{50} concentrations, or with either 250 nM staurosporine (positive control) or vehicle (DMSO), for 8 h, at 37 °C. The culture medium was then removed and cells were washed with HBSS, treated with 0.25% Trypsin-EDTA solution and centrifuged at 390 *g*, for 4 min, to collect the cells as pellet. Afterwards, cells were lysed with a lysis buffer (25 mM Hepes, 5 mM EDTA, 1 mM EGTA, 5 mM $MgCl_2$, 5 mM DTT, pH 7.4, 1% of protease inhibitor cocktail) and subjected to centrifugation at 14 500 *g* for 15 min, at 4 °C. Supernatants (mitochondria-free cytosolic fractions) were collected and the protein concentration was determined by the Bradford method (Kruger, 1994). In order to measure caspase-9 activity, aliquots of mitochondria-free cytosolic fractions containing 50 µg of protein were reconstituted in 150 µL of caspase-9 buffer (25 mM Hepes, pH 7.5, 5 mM DTT, 0.1% CHAPS, and 10% sucrose) supplemented with 50 µM of fluorometric AC-LGHA-AMC caspase-9 substrate (CPC Scientific, CA, USA). Fluorescence was measured in a fluorescent microplate reader (Synergy H1, BioTek) working at an excitation wavelength of 405 nm and an emission wavelength of 535 nm, at different time points, up to 180 min. Results were expressed as fold increase relative to DMSO-treated cells (controls).

2.6.Cell morphology

AGS and SH-SY5Y cells were seeded on coverslips and placed at 37 °C in a CO_2 incubator. After 24 h, cells were treated with dehydroalanine derivatives at IC_{50} concentrations and incubated for 8 h. After this period cells were fixed on coverslips with cold methanol, stained with Giemsa stain and their morphological features were examined under a light microscope (Nikon Eclipse Ci).

2.7. JC-1 Mitochondrial Membrane Potential Assay

AGS and SH-SY5Y cells were seeded in 96-well black plates according to conditions described above for MTT and the Caspase-3/7 assays. Cells were incubated with JC-1 (5,5′,6,6′-tetrachloro-1,1′,3,3′-tetraethyl benzimidazol carbocyanine iodide; Abcam Inc., Cambridge, MA, USA) (7 μM) for 20 minutes, followed by 3 washes with HBSS. For the quantification of mitochondrial membrane potential (ΔΨm), the plate was read using fluorescence microplate reader (Synergy H1, BioTek)) with excitation/emission settings at 485/535 and 560/595 nm, respectively (da Silva et al., 2017). Cells in HBSS were used as negative control and cells treated with 250 μM FCCP, for 30 minutes prior the JC1-addition, were used as a positive control. The ratio of JC-1 aggregate to monomer (the 595:535 ratio) was calculated and a decrease in this ratio was interpreted as ΔΨm depolarization.

2.8.Data analysis

Statistical analysis was carried out by using GraphPad Prism 5. The level of significance between different treatment groups relative to control was determined by one-way analysis of variance (ANOVA), followed by Bonferroni test for between-group comparison. $P < 0.05$ was considered statistically significant. All data were presented as mean ± standard error of the mean (SEM) of three independent experiments, each one performed in triplicate.

3. Results and discussion

This study covered seven *N*-substituted α,β-dehydrophenylalanines, seven α,β-dehydroaminobutyric acid derivatives and five α,β-dehydroalanines, which were prepared using a previously described methodology (Ferreira et al.,1998; Ferreira et al.,1999; Ferreira et al., 2007).

As shown in Table 1, all α,β-dehydroaminoacids derivatives were *N*- and *C*-protected. In all cases the *C*-protection was a methyl ester. Within each group of α,β-dehydroamino acids, the molecular diversity emerges from the chemical structures of the *N*-protecting group. Nine different *N*-protecting groups (one aliphatic and eight with aromatic structures) were used. The library of compound depicted in Table 1 allowed us to study i) the role of the *N*-protecting group on the biological behaviour within each group of α,β-dehydroamino acid derivatives (vertical comparisons), and ii) the impact of a specific *N*-protecting group on the biological properties of different families of α,β-dehydroamino acids (horizontal comparisons).

The presence of a α,β-double bond in the dehydroamino acid residues allows, in the case of dehydrophenylalanine and dehydroaminobutyric acid, the occurrence of *E* and *Z* isomers. Since the molecular configuration has high biological relevance, the selectivity of the synthesis methodology adopted should be taken into account in order to discuss the bioactivity of dehydroaminobutyric acid and dehydrophenylalanine derivatives. The synthesis of these compounds was carried out using a procedure that is stereoselective for the *Z*-isomer (Ferreira et al., 1998; Ferreira et al., 1999; Ferreira et al., 2007). The possible coplanarity of the α,β-double bond with the amide groups, enabling π-electron conjugation that, in some compounds, may be extended up to the aromatic ring of the *N*-protecting group, together with the chemical nature of the *N*-protecting group may dictate a putative impact on the dehydroamino acids chemical and biological behaviour, including on their bioavailability and lipophilicity.

In a first approach considering the compound lipophilicity, the partition coefficient between water and *n*-octanol (Po/w) of each compound was estimated as a sum of fragment-based contributions and correction factors by numerical methods (Molinspiration Cheminformatics software, 2017). The values, expressed as a logarithm

Log P, are presented in Table 1. According to the predicted Log P values, the affinity of all dehydroamino acid derivatives for octanol phase is significantly higher (between one and four orders of magnitude) than for aqueous phase, suggesting their preferential accumulation into the lipid phase of biological systems. It is important to highlight that the log P prediction approach used herein has the potential to process practically all types of organic molecule, as it was validated with 12202 molecules and yielded a good correlation value (R^2 =0.92) between the calculated and the experimentally determined values (http://www.molinspiration.com/services/logp.html). Additionally, it is considered by many researches as a robust methodology to predict realistic Log P values, which are used as quantitative descriptors of compound lipophilicity (Cedrón et al., 2005; Mannhold et al., 2009). Thus, data in Table 1 also show that for the same *N*-protecting group, the lipophilicity of dehydroamino acid derivatives follows the order dehydrophenylalanine > dehydroaminobutyric acid > dehydroalanine, as expected. Considering the partition coefficient values of all dehrydroamino acid derivatives, the plasma membrane (the first physiological barrier encountered by xenobiotics) and the membranes of intracellular compartments (*e.g.* mitochondria) should be the main targets for the putative toxicity of these compounds.

3.1.Cytotoxicity profile of α,β-dehydroaminoacid derivatives

Compounds were screened for their potential as cytotoxicity in three distinct human cancer cell lines, namely A549, AGS and SH-SY5Y cells. These cancer cells were chosen since they are well-established cell models for three human malignant tumour types with high incidence and mortality worldwide (Global Burden of Disease Cancer Collaboration 2016). A549 cell line is a model of non-small cell lung cancer, characterized by a high aggressive phenotype and high resistance to chemotherapeutic

drugs (Lopez-Ayllon et al., 2014). AGS cells are representative of human intestinal-type gastric cancer that also exhibit an evolution pattern of resistance to chemotherapeutic drugs (Jang et al., 2017). SH-SY5Y cells, typically used as a model system to study neuronal development and neurodegenerative diseases, are representative of neuroblastoma tumours that normally are sensitive to chemotherapy, even in advanced stages of disease (Zhang et al., 2016). Thus, a broad spectrum of cancer cell phenotypes, with distinct susceptibility to chemotherapeutic drugs, were used to assess the anticancer activity of the α,β-dehydroamino acid derivatives. Our strategy to screen the cytotoxic activity of these compounds involved, initially, the evaluation of the effects of increasing concentrations (15.625, 31.25 and 62.5 μM) of each dehydroamino acid derivative on the cell viability and plasma membrane integrity of the selected human cancer cell lines. When the effects of those concentrations allowed to predict that a given compound had an IC_{50} smaller than 62.5 μM, additional concentrations of the compound were assessed in order to determine the IC_{50} with higher accuracy.

Figure 1 shows the effects of increasing concentrations of the dehydrophenylalanine derivatives on the viability of A549, AGS and SH-SY5Y cells, after a 24 h incubation period, evaluated by the MTT reduction assay. Dehydrophenylalanine derivatives have limited toxic effects or do not alter the cell viability of these human cancer cell lines. However, data on Figure 1 also revealed that the toxicity of dehydrophenylalanine derivatives depends on the human cancer cell line and on the chemical nature of the *N*-protecting group. A549 cell line is the most sensitive to this type of compounds, since at the highest concentration used (62.5 μM) the dehydrophenylalanine derivatives with an aromatic moiety in the *N*-protecting group significantly decreased cell viability. Toxic effects were detected for the methyl esters of *N*-nitrobenzoyl and *N*-nitrobenzyloxycarbonyldehydrophenylalanine (Phe2 and Phe3, respectively) at 31.25

μM. Differently, SH-SY5Y cells were affected by the methyl ester of *N*-(*tert*-butyloxycarbonyl)-dehydrophenylalanine (Phe9), but not by those derivatives having an aromatic moiety in the *N*-protecting group.

AGS cells viability is significantly reduced by four dehydrophenylalanine derivatives with aromatic protecting groups (Phe2, Phe3, Phe5 and Phe7), the most toxic being the derivative with the toluenesulfonyl group (Tos). The effect of dehydrophenylalanine derivatives on the LDH released into cell culture medium of A549, AGS and SH-SY5Y cells was studied, after 24 h incubation (Figure S1 – supplementary material). No compound caused any detectable effects on the extracellular levels of LDH at the concentration range tested. These data indicate that reduction of cell viability detected by MTT assay is not associated with permeabilization of plasma membrane, and that cytotoxicity of dehydrophenylalanine derivatives does not involve necrosis.

The effects of increasing concentrations of dehydroaminobutyric acid derivatives on the viability of A549, AGS and SH-SY5Y cells, evaluated by MTT assay and by the activity of LDH released into cell culture media, are shown in Figures 2 and S2, respectively. Considering the MTT assay, the dehydroaminobutyric acids present low toxicity for the three human cancer cell lines within the concentration range tested. Data of Figure 2 also suggest that A549 cells are the most resistant, SH-SY5Y cell line being the most sensitive to the effects of dehydroaminobutyric acid derivatives. All compounds were able to promote a significant decrease of the viability of neuroblastoma cells at 62.5 μM, however the reduction of cell viability never exceeded 30%. Considering the biological role of the *N*-group on this type of compounds, it is evident that effects are cell type-dependent. For example, the methyl ester of *N*-benzoyldehydroaminobutyric acid (Abu1) induced toxicity in A549 and SH-SY5Y cells without apparent effects on AGS cells, while the methyl ester of *N*-

quinoxalyldehydroaminobutyric acid (Abu6) affected AGS and SH-SY5Y cells, but not A549 cells.

Figure 3 shows the effects of increasing concentrations of the dehydroalanine derivatives on the viability of the three cell lines, after a 24 h incubation, evaluated by the MTT reduction assay. From the overall data depicted in Figure 3, three remarkable features emerge: i) in the concentration range up to 62.5 μM, all dehydroalanine derivatives significantly decreased the viability of the three human cancer cell lines; ii) for all cancer cell-types used, the cytotoxicity of this group of compounds is significantly higher than that detected for the compounds with the same *N*-protecting group, but belonging to the others dehydroamino acid derivatives; iii) A549 cell line is significantly less sensitive to the effects of dehydroalanine derivatives than AGS and SH-SY5Y cell lines.

Additional concentrations of each dehydroalanine derivative were tested in AGS and SH-SY5Y cells, in order to more accurately assess the IC_{50} values. Considering the IC_{50} values presented in Table 2, the *N*-protecting group has a strong impact on the cytotoxicity of dehydroalanine derivatives. For example, the methyl ester of nitrobenzoyldehydroalanine (Ala2), which has a nitro group in the aromatic ring of the N-acyl group, decreases the IC_{50} from values higher than 62.5 μM to 29.4 μM in AGS cells and to 23.9 μM in SH-SY5Y cells, when compared with the methyl ester of *N*-benzoyldehydroalanine (Ala1).

The toxicity of dehydroalanine derivatives in AGS cells follows the order Ala1 < Ala3 < Ala6 <Ala5 < Ala2, while in SH-SY5Y cells Ala5 switches its position with Ala2 (Ala1 < Ala3 < Ala6 < Ala2< Ala5). Therefore, nitrobenzoyldehydroalanine (Ala2) (IC_{50} of 29.4 μM for AGS and 23.9 μM for SH-SY5Y) and naphthaloyldehydroalanine (Ala5) (IC_{50} of 36.8 μM for AGS and 21.0 μM for SH-SY5Y) are the most toxic

compounds, SH-SY5Y cells being more sensitive to the toxic effects of dehydroalanine derivatives than AGS cells (Fig. 3, table 2).

In order to access selectivity of the molecules towards cancer cells, we have also evaluated the effect of dehydroalanine derivatives on the viability of MRC-5 cells, a non-tumorigenic human lung fibroblast cell line (Figure 4, Table 2). Results show that the MRC-5 cell line, with lower lipid content, is significantly less affected by dehydroalanine derivatives than all cancer cell lines. Only the Ala6 compound exhibits similar toxicity on MRC-5 and A549 cell lines.

Taking into account the structural features of each compound and their toxicity, the capability of the *N*-protecting group to polarize the α,β-double bond seems to be the main factor determining the toxicological profile of α,β-dehydroalanine derivatives. Dehydroalanine derivatives displaying an acyl protecting group (Ala1, Ala2 e Ala5) are considerably more toxic when compared with other protecting groups. Considering the series of compounds *N*-protected with benzoyl, 4-nitrobenzoyl and 4-nitrobenziloxycarbonyl groups (Ala1, Ala2 and Ala3), the dehydroalanine derivative with the most electron withdrawing group attached to nitrogen atom (4-nitrobenzoyl group, Ala 2) is the most toxic, which could be attributed to the polarization of the α,β-double bond through an extended conjugated system with the *N*-protecting group. Also, the increase of toxicity is attained with minor effects on lipophilicity. Conjugation with the *N*-protecting group has an important effect on the toxicity, since the dehydroalanine with the 4-nitrobenzyloxycarbonyl group (Ala3) with one sp^3 carbon atom that breaks the conjugation between the aromatic ring and the amino group is significantly less toxic than Ala2. Regarding dehydroalanines with naphthaloyl (Ala5) and quinoxaloyl (Ala6) groups, they have different effects, the quinoxaloyl derivative being less toxic. Although both groups allow extended conjugation, the quinoxalyl ring is more electron

withdrawing than naphthaloyl, which increases the toxicological potential of Ala6. However, the ability of Ala6 to accumulate into the lipid phase of the biological membranes is much lower than of naphthaloyldehydroalanine (Log P (Ala6) = 0.52, Log P (Ala5) = 2.92). These results suggest that the noxious effects of dehydroalanine derivatives are dependent of both effective membrane concentration of compound (proportional to Log P) and from the ability of the *N*-protecting group to polarize the α,β-double bond. In fact, the higher toxicity of naphthaloyldehydroalanine (Ala5) when compared with benzoyldehydroalanine (Ala1) should also emerge from the greater lipophilic character conferred by naphthalene. Moreover, the susceptibility of these cancer (A549, AGS, SH-SY5Y) and non-cancer (MRC-5) cells to the toxic effects of the *N*-protect dehydroalanine derivatives seems to be directly correlated with their relative content in membrane lipids (Table 2).

In order to investigate whether the loss of cell viability detected by MTT reduction assay is connected with cell death by necrosis, the activity of LDH released into the culture medium of A549, AGS and SH-SY5Y cells was evaluated (Figure S3 supplementary material). In the concentration range tested, the incubation of A549 and AGS cells with dehydroalanine derivatives did not promote any detectable effect on the extracellular levels of LDH, indicating that the toxic effects detected by MTT assay in these cells are not associated with plasma membrane damage. In SH-SY5Y cells, benzoyldehydroalanine (Ala1) and 4-nitrobenzyloxycarbonyldehydroalanine (Ala3) did not affect extracellular LDH activity for all concentrations tested. The same did not happen with concentrations ≥31.25 μM of the compounds with 4-nitrobenzoyl (Ala2) and naphthaloyl (Ala5) groups, or with the highest concentration tested (62.5 μM) of quinoxalyldehydroalanine (Ala6). Therefore, at higher concentrations, Ala2, Ala5 and

Ala6 may induce SH-SY5Y cell death by necrosis, which involves rupture of plasma membrane and increased extracellular LDH activity.

Studies with Ala2, Ala3, Ala5 and Ala6 were extended to gather more information about the cell death pathways triggered by these dehydroalanine derivatives at low concentrations, since they exhibit IC_{50}< 62.5 μM for both AGS and SH-SY5Y cells.

3.2. α,β-Dehydroalanine derivatives trigger morphological changes in cells, caspases activation and mitochondrial membrane depolarization

In order to elucidate the mechanism responsible for the cell death, morphological assessment of cells treated with α,β-dehydroalanine derivatives was carried out**.**

AGS and SH-SY5Y cells were treated with Ala2 and Ala5 at the IC_{50} concentration for 8 h, stained with Giemsa stain and examined under light microscope (Fig. 5). Incubation of AGS and SH-SY5Y cells with Ala2 (Fig 5**b**, **e**) or with Ala5 (Fig. 5**c**, **f**) shows the advent of chromatin condensation, pyknotic nuclei and, in some cases, chromatin fragmentation. These morphological traits are compatible with a process of programmed cell death, reason for which apoptosis was evaluated in subsequent experiments.

Caspases are a family of cysteine dependent aspartate driven proteases that play a key role in the metabolic pathways and signalling networks used by cells to regulate cell death and inflammation, which are fundamental to preserve the functional homeostatic balance of multicellular organisms (McIlwain et al., 2013). Caspases involved in apoptosis are normally sorted as initiator caspases (caspase-8 and -9, associated with extrinsic and intrinsic pathways, respectively) and executioner caspases (caspase-3, -6 and -7) that are the effective players of the characteristic morphological events of apoptosis (Pereira et al., 2014). Caspase-4, initially associated with the regulation of the

inflammatory process, is now also considered to be a key player of apoptosis triggered by endoplasmic reticulum stress (Pereira et al. 2015; Bian et al., 2009).

In order to evaluate whether the selected dehydroalanine derivatives are able to induce cancer cell apoptosis, the proteolytic cleavage activity of caspases-3/7, caspases-9 and caspase-4 was assessed in AGS and SH-SY5Y cell lines, 8 h after cell incubation with compounds at IC_{50} concentrations (Fig. 6).

As shown in Figure 6**a** and 5**d**, the selected dehydroalanine derivatives promote a significant increase of the activity of caspases-3/7 in both AGS and SH-SY5Y cell lines. In AGS cells, the effects on caspase 3/7 activity are similar for all dehydroalanine derivatives. Thus, the intensity of the effects in neuroblastoma cells seems to be dependent of the *N*-protecting group, following the order Ala2 > Ala5 > Ala6 ≥ Ala3.

Regarding the initiator caspase of the intrinsic or mitochondrial pathway, data on Figure 6**b** show that the proteolytic cleavage activity of caspase-9 in AGS cells incubated with the compounds is higher than in control cells. However, the differences did not reach statistical significance, suggesting that the apoptotic running detected in AGS cells by the increased caspases-3/7 activity did not proceed from caspase-9 activation, usually associated to the mitochondrial pathway of apoptosis. In fact, Ala2, Ala5 and Ala6 were able to promote a significant increase of caspase-4 proteolytic cleavage activity, a caspase connected not only with inflammasome activation, but also with programmed cell death via endoplasmic reticulum-stress pathway (Pereira et al., 2015), as shown in Figure 6**c**. Thus, the endoplasmic reticulum may be the main toxicological target of dehydroalanine derivatives in intestinal-type gastric cancer cells.

On the other hand, in SH-SY5Y cells dehydroalanine derivatives did not promote any detectable effects on the activity of caspase-4 (Fig. 6**f**). Furthermore, only compound Ala2 was able to induce a significant increase of proteolytic cleavage activity of

caspase-9 (Fig. 6**e**). Since the activation of upstream caspase-9 leads to the proteolytic activation of the downstream or effector caspases-3/7 (McIlwain et al., 2013), Ala2 may induce SH-SY5Y cells apoptosis through the mitochondrial pathway. In relation to cell death pathways triggered by Ala3, Ala5 and Ala6 dehydroalanine derivatives in SH-SY5Y cells, our data did not support any preferential pathway. However, it is important to stress that during apoptotic cell death, caspases are sequentially activated in a self-amplifying cascade and the duration of an apoptotic run, dependent of cell type, was estimated to change between 6 and 24 h [Gravrieli et al., 1992].

Considering that the loss of mitochondrial membrane potential ($\Delta\Psi m$) is a typical feature of apoptotic cells (Zamzami and Kroemer, 2001), the influence of Ala2, Ala3, Ala5 and Ala6 on $\Delta\Psi m$ of AGS and SH-SY5Y cells was evaluated (Figure 7). The ratio of the fluorescent probe JC-1 aggregate to monomer is directly proportional to $\Delta\Psi m$, since mitochondrial accumulation of the membrane-permeable cationic probe is governed by Nernst equation. Dehydroalanine derivatives promoted a significant decrease of $\Delta\Psi m$ in both AGS and SH-SY5Y cell lines, being Ala6 the most efficient for both cell lines. Thus, the effects of these molecules upon $\Delta\Psi m$ are in agreement with the results described before in morphological assessment and caspases activity. Nevertheless, the activation of death receptors in plasma membrane (extrinsic pathway) and cell autophagy are other possibilities not investigated in the present work.

4. Conclusions

The present work describes for the first time the biological activity of α,β-dehydroamino acid derivatives on three human cancer cell lines, representatives from lung (A549), gastric (AGS) and neuroblastoma (SH-SY5Y) tumours. Chemical screening revealed four α,β-dehydroalanine derivatives with significant cytotoxic

effects (IC_{50}< 62.5 μM) on both AGS and SH-SY5Y cells. The analysis of structure-activity relationships suggests the lipophilic character of dehydroalanine derivatives associated with the electron withdrawing effect of the *N*-protecting group are the main factor determining the toxicity of α,β-dehydroalanine derivatives. Additionally, the selected compounds trigger a process of programmed cell death compatible with apoptosis, putatively endoplasmic reticulum-dependent in the case of AGS cells and mitochondria-dependent in SH-SY5Y cells. Considering that many pharmacological drugs used in cancer treatment have the induction of apoptosis and/or cell cycle arrest as a primary goal (Makin and Dive, 2001; Wong, 2001), α,β-dehydroalanine derivatives (*e.g*. Ala2 and Ala5) that are able to kill both AGS and SH-SY5Y cells (IC_{50}< 30 μM) through the induction of apoptosis may be potential resources for coping with human intestinal-type gastric cancer and neuroblastoma tumours.

Acknowledgments

This work received financial support from National Funds (FCT/MEC) through project UID/QUI/50006/2013, co-financed by European Union (FEDER under the Partnership Agreement PT2020); and from Norte Portugal Regional Operational Programme (NORTE 2020), under the PORTUGAL 2020 Partnership Agreement, through the European Regional Development Fund (ERDF) (project NORTE-01-0145-FEDER-000024).

Supplementary information

Figure S1. Activity of LDH released into the culture medium of A549, AGS and SH-SY5Y cells, incubated for 24 h with increasing concentrations of α,β-dehydrophenylalanine derivatives.

Figure S2. Activity of LDH released into culture medium of A549, AGS and SH-SY5Y cells, incubated for 24 h, with increasing concentrations of α,β-dehydro-2-aminobutyric acid derivatives.

Figure S3. Activity of LDH released into culture medium of A549, AGS and SH-SY5Y cells, incubated for 24 h with increasing concentrations of α,β-dehydroalanine derivatives.

References

Arnison, P.G.; Bibb, M.J.; Bierbaum, G.; Bowers, A.A.; Bugni, T.S.; Bulaj, G.; Camarero, J.A.; Campopiano, D.J.; Challis, G.L.; Clardy, J.; *et al.* Ribosomally synthesized and post-translationally modified peptide natural products: overview and recommendations for a universal nomenclature. *Nat. Prod. Rep*. **2013**, 30, 108-160. https://www.ncbi.nlm.nih.gov/pubmed/23165928

Bian, Z.-M.; Elner, S.G.; Elner, V.M. Dual involvement of Caspase-4 in Inflammatory and ER Stress-induced Apoptotic Responses in Human Retinal Pigment Epithelial Cells. *Invest. Ophthalmol. Vis. Sci.* **2009**, 50(12), 6006–6014. http://doi.org/10.1167/iovs.09-3628

Bonnard, I.; Rolland, M.; Salmon, J.-M. Debiton, E.; Barthomeuf, C.; Banaigs, B. Total structure and inhibition of tumour cell proliferation of laxaphycins. *J. Med. Chem*. **2007**, 50, 1266–1279. http://pubs.acs.org/doi/abs/10.1021/jm061307x

Cedrón, J.C.; Ravelo, Á.G.; León, L.G.; Padrón, J.M.; Estévez-Braun, A. Antiproliferative and Structure Activity Relationships of Amaryllidaceae Alkaloids. *Molecules*. **2015**, 20, 13854-13863. http://doi.org10.3390/molecules200813854

da Silva, D.C.; Andrade, P.B.; Valentão, P.; Pereira D.M. Neurotoxicity of the steroidal alkaloids tomatine and tomatidine is RIP1 kinase- and caspase-independent and involves the eIF2a branch of the endoplasmic reticulum. *J. Steroid Biochem. Mol. Biol.* **2017**, 171, 178-186. https://www.ncbi.nlm.nih.gov/pubmed/28300624

Ferreira, P.M.T.; H.L.S. Maia; Monteiro, L.S. Electrochemical synthesis of diaminodicarboxylic acid derivatives. *Tetrahedron Lett.* **2003**, 44, 2137-2139. http://doi.org/10.1016/S0040-4039(03)00163-1

Ferreira, P.M.T.; Maia, H.L.S.; Monteiro, L.S. Efficient synthesis of dehydroamino acid derivatives. *Tetrahedron Lett*. **1998**, 39(51), 9575-9578. https://doi.org/10.1016/S0040-4039(98)02164-9

Ferreira, P.M.T.; Maia, H.L.S.; Monteiro, L.S.; Sacramento, J. High yielding synthesis of dehydroamino acid and dehydropeptide derivatives. *J. Chem. Soc., Perkin Trans.1,* **1999,** 3697-3703. https://doi.org/10.1039/A904730A

Ferreira, P.M.T.; Maia, H.L.S.; Monteiro, L.S.; Sacramento, J. Michael addition of thiols, carbon nucleophiles and amines to dehydroamino acid and dehydropeptide derivatives. *J. Chem. Soc., Perkin. Trans.* **2001**, 1, 3167-3174. http://doi.org/10.1039/b106487h

Ferreira, P.M.T.; Maia, H.L.S.; Pereira, G. Reactivity of dehydroamino acids and dehydrodipeptides towards *N*-bromosuccinimide: synthesis of β-bromoand β,β-dibromodehydroamino acid derivatives and of substituted 4-imidazolidinones. *Eur. J. Org. Chem.* **2007**, 35, 5934-5949. https://doi.org/10.1002/ejoc.200700669

Ferreira, P.M.T.; Monteiro, L.S.; Pereira, G. Synthesis of substituted oxazoles from *N*-acyl-β-hydroxyamino acid derivatives. *Eur. J. Org. Chem.* **2008**, 4676-4683. https://doi.org/10.1002/ejoc.200800602

Global Burden of Disease Cancer Collaboration 2016. Global, Regional, and National Cancer Incidence, Mortality, Years of Life Lost, Years Lived With Disability, and Disability-Adjusted Life-years for 32 Cancer Groups, 1990 to 2015A Systematic Analysis for the Global Burden of Disease Study. *JAMA Oncol*. **2016**, Published online December 03, 2016. http://doi.org/10.1001/jamaoncol.2016.5688

Gravrieli, Y.; Sherman, Y.; Ben-Sasson, S.A. Identification of programmed cell death in situ via specific labelling of nuclear DNA fragmentation. *J. Cell Biol*. **1992**, 119, 493-501. http://dx.doi.org/10.1083/jcb.119.3.493

Gupt,a M.; Chauhan, V.S. De novo design of α,β-didehydrophenylalanine containing peptides: From models to applications. *Biopolymers*, **2011**, 95, 161–173. http://doi.org/10.1002/bip.21561

Jang, M.; Koh, I.; Lee, S.J.; Cheong, J.H.; Kim, P. Droplet-based microtumor model to assess cell-ECM interactions and drug resistance of gastric cancer cells. *Sci. Rep.*, **2017**, 7, 41541. http://doi.org/10.1038/srep41541

Kruger, N.J. The Bradford method for protein quantitation. *Methods Mol. Biol.* **1994**, 32:9-15. https://doi.org/10.1385/0-89603-268-X:9

Lopez-Ayllon, B.D.; Moncho-Amor, V.; Abarrategi, A.; de Cáceres, I.I.; Castro-Carpeño, J.; Belda-Iniesta, C; Sastre, L. Cancer stem cells and cisplatin-resistant cells isolated from non-small-lung cancer cell lines constitute related cell populations. *Cancer Med.*, **2014**, *3*(5), 1099–1111. http://doi.org/10.1002/cam4.291

Mannhold, R.; Poda, G.I.; Ostermann, C.; Tetko, I.V. Calculation of molecular lipophilicity: State-of-the-art and comparison of log P methods on more than 96,000 compounds. *J. Pharm. Sci*. **2009,** 98(3):861-93. https://www.ncbi.nlm.nih.gov/pubmed/18683876

Makin, G.; Dive, C. Apoptosis and cancer chemotherapy, *Trends Cell Biol*., **2001**, 11(11), S22-S26. http://dx.doi.org/10.1016/S0962-8924(01)02124-9

McIlwain, D.R.; Berger, T.; Mak, T.W. Caspase Functions in Cell Death and Disease. *Cold Spring Harb. Perspect. Biol.* **2013**, *5,a008656*. http://doi.org/10.1101/cshperspect.a026716

Monteiro-Cardoso, V.F.; Silva, A.M.; Oliveira, M.M.; Peixoto, F.; Videira, R.A. Membrane lipid profile alterations are associated with the metabolic adaptation of the Caco-2 cells to aglycemic nutritional condition. *J. Bioenerg. Biomembr*. **2014**, 46(1), 45-57. https://link.springer.com/article/10.1007%2Fs10863-013-9531-y

Morrison, P.M.; Foley, P.J.; Warriner, S.L.; Webb, M.E. Chemical generation and modification of peptides containing multiple dehydroalanines. *Chem. Commun.* **2015**, 51, 13470-13473. https://www.ncbi.nlm.nih.gov/pmc/articles/PMC4847484/

Okeley, N.M.; Zhu, Y.; van Der Donk, W.A. Facile chemoselective synthesis of dehydroalanine-containing peptides. *Org. Lett*. **2000**, 2(23), 3603-3606. http://pubs.acs.org/doi/abs/10.1021/ol006485d

Pereira, D.M.; Correia-da-Silva, G.; Valentão, P.; Teixeira, N.; Andrade, P.B. Palmitic Acid and Ergosta-7,22-dien-3-ol Contribute to the Apoptotic Effect and Cell Cycle Arrest of an Extract from *Marthasteriasglacialis L.* in Neuroblastoma Cells. *Marine Drugs,* **2014**, 12(1), 54–68. http://doi.org/10.3390/md12010054

Pereira, D.M.; Valentão, P.; Correia-da-Silva, G.; Teixeira, N.; Andrade, P.B. Translating endoplasmic reticulum biology into the clinic: a role for ER-targeted natural products? *Nat. Prod. Rep*. **2015**, 32, 705-722. http://doi.org/10.1039/C4NP00102H

Pereira, D.M.; Valentão, P.; Correia-da-Silva, G.; Teixeira, N.; Andrade, P.B. (). Plant secondary metabolites in cancer chemotherapy: Where are we? *Curr. Pharm. Biotechnol*. **2012,** 13, 632–650. http://doi.org/10.2174/138920112799857530

Repka, L.M.; Chekan, J.R.; Nair, S.K.; van der Donk, W.A. Mechanistic Understanding of Lanthipeptide Biosynthetic Enzymes. *Chem. Rev.* Article ASAP. **2017**, http://pubs.acs.org/doi/abs/10.1021/acs.chemrev.6b00591

Rudresh; Ramakumar, S.; Ramagopal, U.A.; Inai, Y.; Goel, S.; Sahal, D., Chauhan, V.S. De novo design and characterization of a helical hairpin eicosapeptide; Emergence of an anion receptor in the linker region. *Structure*, **2004**, 12(3), 389-396. http://doi.org/10.1016/j.str.2004.02.014

Siodłak, D. α,β-Dehydroamino acidsin natural occurring peptides. *Amino Acids*, **2015**, 47: 1–17. http://doi.org/10.1007/s00726-014-1846-4

Ward, D.E.; Vazquez, A., Pedras, M.S.C. Probing host-selective phytotoxicity: synthesis and biological activity of phomalide, isophomalide, and dihydrophomalide. *J. Org. Chem.* **1999**, 64, 1657–1666. http://pubs.acs.org/doi/abs/10.1021/jo982376p

Wong, R.S.Y. Apoptosis in cancer: from pathogenesis to treatment. *J. Exp. Clin. Canc. Res.* **2011**, 30:87, 1-14. http://dx.doi.org/10.1186/1756-9966-30-87

Zamzami, N.; Kroemer, G. The mitochondrion in apoptosis: how Pandora's box opens. *Nat. Rev. Mol. Cell Biol.* **2001**, 2(1), 67-71. https://www.ncbi.nlm.nih.gov/pubmed/11413468

Zhang, Y.; Huang, D.; Zhang, W.; Tang, S.; Han, T.; Zhu, X.; Zhi, T. Clinical characteristics of infant neuroblastoma and a summary of treatment outcome. *Oncol. Lett.* **2016**, *12*(6), 5356-5362. http://doi.org/10.3892/ol.2016.5353

Table 1. Library of *N*-protected α,β-dehydroamino acids derivatives used in the present study. General structure, designation (Nº), structure of the *N*-substituent group (R) and logarithm of the partition coefficient between water and *n*-octanol (Log P).

α,β-dehydrophenylalanine derivatives			α,β-dehydroaminobutyric acid derivatives			α,β-dehydroalanine derivatives		
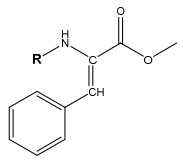			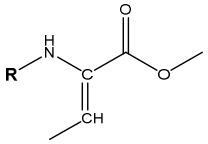			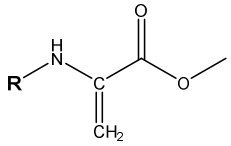		
Nº	(R) **Structure/ name**	**Log P**	**Nº**	(R) **Structure/name**	**Log P**	**Nº**	(R) **Structure/name**	**Log P**
Phe1	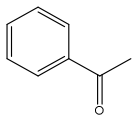 Bz-ΔPhe-OMe	3.45	**Abu1**	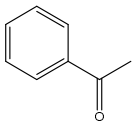 Bz-ΔAbu-OMe	2.00	**Ala1**	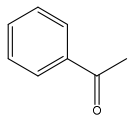 BzΔAla-OMe	1.75
Phe2	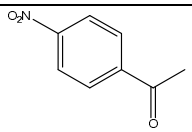 Bz(NO_2)-ΔPhe-OMe	3.41				**Ala2**	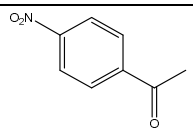 Bz(NO_2)-ΔAla-OMe	1.71
Phe3	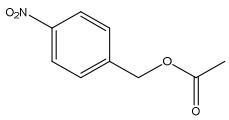 Z(NO_2)-ΔPhe-OMe	3.82	**Abu3**	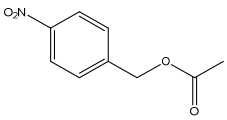 Z(NO_2)-ΔAbu-OMe	2.37	**Ala3**	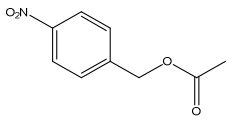 Z(NO_2)ΔAla-OMe	2.12
Phe4	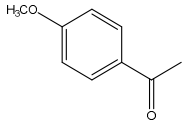 Bz(OMe)-ΔPhe-OMe	3.41	**Abu4**	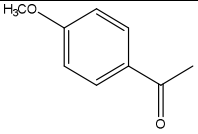 Bz(OMe)ΔAbu-OMe	2.05			
Phe5	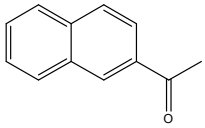 Naph-ΔPhe-OMe	4.64	**Abu5**	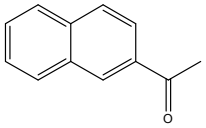 Naph-ΔAbu-OMe	3.18	**Ala5**	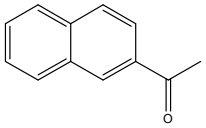 Naph-ΔAla-OMe	2.93
			Abu6	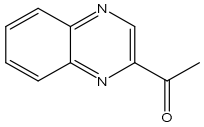 Qnx-ΔAbu-OMe	2.03	**Ala6**	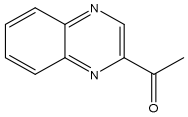 Qnx-ΔAla-OMe	0.52
Phe7	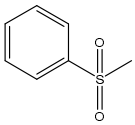 Tos-ΔPhe-OMe	3.78	**Abu7**	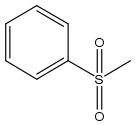 Tos-ΔAbu-OMe	2.32			
			Abu8	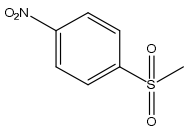 Nosil-ΔAbu-OMe	1.83			
Phe9	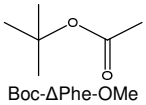 Boc-ΔPhe-OMe	3.45						

Table 2. Membrane lipid parameters of total lipid extract obtained from cancer (A549, AGS and SH-SY5Y) and non-cancer (MRC-5) cells; and IC_{50} values of the *N*-protected α,β-dehydroalanine derivatives assessed in A549, AGS, SH-SY5Y and MRC-5 cell lines by MTT assay.

	A549	**AGS**	**SH-SY5Y**	**MRC-5**
Phospholipid content (nmol/ mg of protein)	269.2±19.6	352.8±32.6	391.7±36.7	155.7±14.8
Cholesterol content (nmoles/mg of protein)	67.8±6.2	108.9±27.7	118.9±37.6	52.6±4.6
α,β-dehydroalanine derivatives / Nº	**IC_{50}** (μM)	**IC_{50}** (μM)	**IC_{50}** (μM)	**IC_{50}** (μM)
Ala1	>62.5	>62.5	>62.5	>62.5
Ala2	>62.5	29.4	23.9	>62.5
Ala3	>62.5	60.3	62.3	>62.5
Ala5	>62.5	36.8	21.0	>62.5
Ala6	>62.5	54.6	42.4	>62.5

Legend to the Figures

Figure 1. Cytotoxicity of α,β-dehydrophenylalanine derivatives in A549, AGS and SH-SY5Y cells. Cell viability was assessed by the MTT reduction assay after a 24 h incubation period, as described in Materials and Methods. Results are expressed as percentage of control (cells treated with vehicle) and presented as mean ± standard error of mean (SEM) of, at least, three independent experiments, each one performed in triplicate. Comparisons relative to the control were performed using one-way ANOVA with Bonferroni as post-test (*$p < 0.05$; **$p < 0.01$; ***$p < 0.001$).

Figure 2. Cytotoxicity of α,β-dehydroaminobutyric acid derivatives in A549, AGS and SH-SY5Y cells. Cell viability was assessed by the MTT reduction assay after 24 h incubation period, as described in Materials and Methods. Results are expressed as percentage of control (cells treated with vehicle) and presented as mean ± standard error of mean (SEM) of, at least, three independent experiments, each one performed in triplicate. Comparisons relative to the control were performed using one-way ANOVA with Bonferroni as post-test (*$p < 0.05$; **$p < 0.01$; ***$p < 0.001$).

Figure 3. Cytotoxicity of α,β-dehydroalanine derivatives in A549, AGS and SH-SY5Y cells. Cell viability was assessed by the MTT reduction assay after 24 h incubation period, as described in Materials and Methods. Results are expressed as percentage of control (cells treated with vehicle) and presented as mean ± standard error of mean (SEM) of, at least, three independent experiments, each one performed in triplicate. Comparisons relative to the control were performed using one-way ANOVA with Bonferroni as post-test (*$p < 0.05$; **$p < 0.01$; ***$p < 0.001$).

Figure 4. Cytotoxicity of α,β-dehydroalanine derivatives in MRC-5 cells. Cell viability was assessed by the MTT reduction assay after 24 h incubation period, as described in Materials and Methods. Results are expressed as percentage of control (cells treated with vehicle) and presented as mean ± standard error of mean (SEM) of, at least, three independent experiments, each one performed in triplicate. Comparisons relative to the control were performed using one-way ANOVA with Bonferroni as post-test (***$p < 0.001$).

Figure 5. Morphological assessment of Giemsa stained AGS (**a**, **b**, **c**) and SH-SY5Y (**d**, **e**, **f**) cells, evaluated by light microscopy, without (**a**, **d**) and after treatment with Ala2 (**b**, **e**) or Ala5 (**c**, **f**) α,β-dehydroalanine derivatives, at IC_{50} concentrations, for 8 h. Giemsa staining shows chromatin condensation (green arrows) and fragmentation (red arrows).

Figure 6. Effect of α,β-dehydroalanine derivatives (Ala2, Ala3, Ala5 and Ala6) at IC_{50} concentrations on the proteolytic cleavage activity of caspases-3/7 (**a**, **d**), caspase-9 (**b**, **e**) and caspase-4 (**c**, **f**) of AGS (**a**, **b**, **c**) and SH-SY5Y cells (**d**, **e**, **f**). Results are expressed as fold increase relative to DMSO-treated cells (control) and presented as mean ± standard error of mean (SEM) of three independent experiments, each one performed in duplicate. Staurosporine (250 nM) was used as positive control for caspase-3/7 and caspase-9 and palmitic acid (1 mM) for caspase-4. Comparisons relative to the control were performed using one-way ANOVA with Bonferroni as post-test (*$p < 0.05$; **$p < 0.01$; ***$p < 0.001$).

Figure 7. Effect of α,β-dehydroalanine derivatives (Ala2, Ala3, Ala5 and Ala6) at IC_{50} concentrations on mitochondrial transmembrane potential of AGS and SH-SY5Y cells, evaluated by using the dual-emission potential-sensitive JC-1 probe. Results are expressed by ratio of red (aggregate) to green (monomer) fluorescence JC-1, and presented as mean ± standard error of mean (SEM) of three independent experiments, each one performed in triplicate. FCCP (250 nM) was used as positive control. Comparisons relative to the control were performed using one-way ANOVA with Bonferroni as post-test ***$p < 0.001$).